

## Joint Inversion of Direct Current and Electromagnetic Soundings

\*Henry Ekene Ohaegbuchi, Boniface Ikechukwu Ijeh and Marry Ihechiluru. Ojiaku

Received: 14 September 2022/Accepted 11 March 2023/Published online: 15 March 2023

**Abstract:** *It was necessary to first build equivalent synthetic datasets to concurrently invert direct current (DC) and frequency-domain electromagnetic (FDEM) soundings. Declaring the initial number of subsurface layers, the spacing between the AB/2 and MN/2 electrodes, the range of acceptable frequencies, and the coil spacing employed to achieve this. Therefore, using these characteristics, we were able to create DC resistivity and FDEM data that resemble the actual field data that was previously obtained by traditional geophysical surveys. The DC and FDEM datasets were each given 3% and 1% of Gaussian white noise, with regularization strengths of 500 and 300, respectively. Across a homogeneous half-space with three layers and a thickness of 15 m, this was defined. We started a model transformation after creating the synthetic data, which turned the data into logarithms with upper and lower bounds. The DC and FDEM datasets were then independently inverted for comparison with their joint inversion. A combined forward operator was subsequently developed that takes into account the unique characteristics of the various geophysical datasets. By integrating the datasets, transformations, and related errors, we were able to invert the DC and FDEM jointly using the joint forward operator. When the combined inversion's results were shown side by side with the results from the separate inversions, it was found that the joint inversion offered a more accurate picture of the subsurface (model) as the computational errors were much less than that associated with the separate inversions of the individual geophysical datasets.*

**Keywords:** *Joint inversion, resistivity, frequency-domain, electromagnetics, synthetic datasets.*

**Henry Ekene Ohaegbuchi**

Department of Physics  
College of Physical and Applied Sciences  
Michael Okpara University of Agriculture,  
Umudike, Abia State, Nigeria.

**Email:** [eo.henry@mouau.edu.ng](mailto:eo.henry@mouau.edu.ng)

**Orcid id:** 0000-0002-8269-8830

**Boniface Ikechukwu Ijeh**

Department of Physics  
College of Physical and Applied Sciences  
Michael Okpara University of Agriculture,  
Umudike, Abia State, Nigeria.

**Email:** [Ijeh.ikechukwu@mouau.edu.ng](mailto:Ijeh.ikechukwu@mouau.edu.ng)

**Orcid id:** 0000-0002-2617-5314

**Marry Ihechiluru. Ojiaku** Department of Physics

College of Physical and Applied Sciences  
Michael Okpara University of Agriculture,  
Umudike, Abia State, Nigeria.

**Email:** [maryihechiluru31@gmail.com](mailto:maryihechiluru31@gmail.com)

**Orcid id:** 0009-0004-2344-2378

### 1.0 Introduction

Direct current is the term used to describe an electrical current that flows in one direction and has a relatively constant magnitude. To gather data from gradually deeper depths at a specific surface position, a direct current resistivity or IP approach with increased electrode spacing can be used (Appa-Rao and Roy, 1973).

Electromagnetism is the study of telluric current, ionosphere, terrestrial magnetism, and atmospheric electricity. An

**Corresponding Author:** H. E. Ohaegbuchi, Email: [eo.henry@mouau.edu.ng](mailto:eo.henry@mouau.edu.ng)

electromagnetic method, which typically assumes horizontal stacking, is designed to identify changes in electrical conductivity with depth. Using a fixed source and receiver, measurements are typically taken at a variety of frequencies (in frequency domain sounding). By adjusting the distance between the source and the receiver, sounding can also be produced at a constant frequency.

Electric current flow in the earth causes surface effects, which are detected using electrical geophysical prospecting methods. Potentials, currents, and electromagnetic fields that are present naturally or artificially in the ground can all be measured using electrical techniques (Buselli et al., 1990). The electrical resistance of the ground between the probes is determined by the potential difference for a unit current passed through the ground. The resistance depends on the electrodes' geometrical arrangement and the electrical characteristics of the ground (Nabighian, 1991; Zhdanov, M.S. and Keller, 1994).

For both the planning and interpretation of electromagnetic (EM) sounding experiments, an estimation of the depth of study is essential. Petroleum, mineral, groundwater, and geothermal exploration all use electromagnetic (EM) sounding, which comprises controlled-source techniques (both frequency and time-domain) and natural-source techniques like magnetotellurics (Keller, 1992). The depth of a buried inhomogeneity's burial and the average conductivity of the section above it determine when or at what frequency the inhomogeneity's electromagnetic (EM) response can be first measured; the type of source or receiver and how far apart they are from one another are relatively unimportant factors (Verma and Sharma, 1993). The sensitivity and precision of the instrumentation, the strength of the signal, and the amount of noise, however, all affect the capacity to make measurements at this time or frequency (Verma and Mallick, 1979). Geoelectrical techniques are extensively used in the sectors of engineering and mineral prospecting and each technique has pros and

cons when it comes to determining the depths and electrical characteristics of the underlying subsurface. Based on available information from several literature, the combination of sounding data from different methodologies has been proven to be an efficient way to increase the dependability of interpretation. Among them, several authors created intriguing schemes to simultaneously invert two sounding data obtained from two different surveying techniques, such as gravity gradiometry and magnetotelluric (MT) data (Zhang and Li, 2019) and transient electromagnetic (TEM) and full-waveform seismic data (Gao *et al.*, 2012) into geoelectric sections. By simultaneously inverting synthetic frequency-domain electromagnetic (FDEM) and direct current (DC) data, this study expands on their previous work.

## 2.0 Methodology

The Python programming language will be used to create a program for this investigation, which aims to maximize more desirable information about the subsurface by combining direct current and electromagnetic data. This would be able to provide artificial electromagnetic and direct current data that would be identical to data that could be obtained from a field survey. These artificial data would then be inverted collectively to produce a model of the subsurface's makeup. Here, we outline the equipment needed to do a joint inversion of data from small-loop electromagnetic (EM) and direct current (DC) resistivity measurements. The two forward models used to explain the relationship between electrical conductivity (EC), DC resistivity, and electromagnetic (EM) data are specifically mentioned here, as are the inversion technique—in this case, the Geophysical Inversion & Modelling Library in a Python environment—and the two forward models themselves.

### 2.1. Frequency-Domain Electromagnetics

There are numerous alternative measuring setups for EM data, and each of them is susceptible to the subsurface EC. The small



loop-loop frequency-domain electromagnetic (FDEM) induction method is the EM technique covered in this study. When small-loop FDEM techniques are used, a primary electromagnetic field is created by an alternating current of a single low frequency, in this case 9 kHz, in a transmitter coil that is roughly analogous to a magnetic dipole. A diffusion equation provided below, can be used to characterize the ensuing EM field propagation.

$$E(r, t) \approx \frac{I_0 l}{4\pi\sigma r^3} \left[ f_1\left(\frac{t}{t_d}\right) \hat{\theta} \sin\theta + f_2\left(\frac{t}{t_d}\right) (\hat{\theta} \sin\theta + 2\hat{r} \cos\theta) \right] \quad (1)$$

$$H(r, t) \approx \frac{I_0 l}{4\pi r^2} f_2\left(\frac{t}{t_d}\right) \hat{\phi} \sin\theta, \quad (2)$$

where

$$f_1(x) = \frac{4}{\sqrt{\pi} x^3} \exp\left(\frac{-1}{x}\right) \quad (3)$$

is the far-field step response for the electrical field and

$$f_2(x) = 1 + \frac{2}{\sqrt{\pi} x^3} \exp\left(\frac{-1}{x}\right) - \operatorname{erf}\left(\frac{1}{\sqrt{x}}\right) \quad (4)$$

is the step response of the two near-field terms for the electric field. For convenience, the dipole step responses are expressed in terms of a scaled time  $x = t/t_d$ , where  $t_d = \mu\sigma r^2/4$  and  $r$  a radius vector.

In conductive material that is impacted by the primary field, this field causes eddy currents. The secondary magnetic field is produced by these eddy currents. With one or more receiver coils positioned at a specific distance from the transmitter coil, the secondary field is recorded alongside the primary field. The measurement sensitivity is highly dependent on the various coil geometries in addition to the transmitter-receiver offset. The subsurface EC, the measurement quantity of interest, and the secondary field's strength can be connected. The secondary field is often expressed in parts-per-million [ppm] as in-phase (IP) and quadrature-phase (QP) components concerning the primary field.

In this study, we simulate FDEM data by applying the physical equations given by equations 1–4 in a Python environment using the code associated with the Geophysical

Inversion & Modelling Library. Their explanation indicates a non-linear relationship between the measurement and electrical conductivity of the subsurface volume influenced by the induction phenomenon using a one-dimensional full solution of Maxwell's equations. Little loop-loop FDEM field data are known to have significant systematic errors. To adapt the FDEM forward model for the field data application detailed in this study, we simply added an offset term to the QP and IP answers. These offsets serve as a reminder of any potential systemic faults present in the IP and QP answers.

## 2.2 Vertical Electrical Sounding

At the earth's surface, direct current resistivity measurements are often taken using a four-point electrode setup. In such a setup, one set of current electrodes injects a specific amount of current into the ground while a second set of electrodes records the voltage that results. We will use the Schlumberger vertical electrical sounding (VES) setup in this work because it is frequently applied for the investigation of vertical variation in EC and, consequently, frequently used in one-dimensional EC modeling of the subsurface. For Schlumberger VES measurements, the pair of voltage electrodes remains fixed in alignment with the current electrodes, and after each voltage measurement, the space between the current electrodes is widened. The recorded voltage can be represented as apparent electrical conductivity by applying Ohm's law and assuming that the entire subsurface is a homogeneous half-space (EC). The spatial distribution of the subsurface electrical conductivity distribution is related to the apparent EC. Ohaegbuchi et al(2019) 's full explanation of the VES forward model utilized provides the apparent resistivity of the subsurface as

$$\rho_a = \pi \left[ \frac{s^2}{a} - \frac{a}{4} \right] \frac{V}{I}, \quad (5)$$

where  $a$  is the inner (potential) electrode spacing and  $s$  is the outer (current) electrode spacing,  $V$  and  $I$  are the potential difference and current respectively.



### 2.3 Joint inversion of DC and FDEM data

Using the Geophysical Inversion & Modelling Library in a Python context, the direct current (DC) and frequency-domain electromagnetic (FDEM) data are jointly inverted. In the latter case, a two-coil system with 10 frequencies between 110 Hz and 56 kHz is assumed to be horizontally coplanar. The FDEM results are reported as the ratio between the secondary and primary fields in percent or parts per million, whereas DC resistivity produces apparent resistivities (ppm).

Since they both employ the same block model, the two ready methods DC1dModelling and FDEM1dModelling can be merged quite quickly. The two vectors are combined in the response function. A new modelling class that we developed has two members of the individual classes and derives from the base modelling class 12; these elements must be initialized in the constructor. Alternatively, we could only utilize a member of the other class while deriving from one of the two classes.

The import command is used to call both response functions in the response function and combine them. The normal inversion and transformation settings (log for apparent resistivity and logLU for the resistivity) are

used. This would be the entire situation in the case of similar responses (such as apparent resistivities). Here, we must take into consideration the various data kinds, including the usually positive, log-distributed relative magnetic fields from DC and maybe the negative, linearly distributed ones. CumulativeTrans is once more used to combine the transformations. We establish a synthetic model called synthModel in the code, compute the forward response, and then modify it using the specified noise levels. We fitted the data within error boundaries as the inversion converges to a value of approximately 1.

The final step is to conduct a resolution analysis to evaluate the accuracy of the determination of the individual parameters (three resistivities and two thicknesses). By dramatically raising the error level for one of the approaches by a factor of 10, we may contrast it with single inversions. The resolution matrix's diagonal values for a three-layer model are displayed in Table 1. Except for the first layer resistivity for FDEM, the first layer is highly resolved in all variations. When we take into account the values for the other resistivities, it is evident that DC describes the resistor as anticipated by theory while FDEM detects the excellent conductor.

**Table 1: Resolution measures for joint inversion and single inversions using an error model increased by a factor of 10.**

Method	$d_1 = 20$ m	$d_2 = 20$ m	$\rho_1 = 200$ $\Omega$ m	$\rho_2 = 10$ $\Omega$ m	$\rho_3 = 50$ $\Omega$ m
Joint inversion	0.98	0.46	0.98	0.67	0.57
FDEM dominated	0.97	0.36	0.71	0.66	0.2
DC dominated	0.96	0.21	0.97	0.32	0.62

### 3.0 Results and Discussion

Here, we show the outcomes of a combined inversion utilizing the Python environment and the Geophysical Inversion & Modelling Library. Also, we contrasted the outcomes of the separate inversions of DC resistivity and FDEM data with the outcomes of the

combination inversions. The first is the final subsurface model, which is depicted in Fig. 1 below and displays the resistivity predictions made using synthetic datasets from DC, FDEM, and the joint inversion as a function of depth.



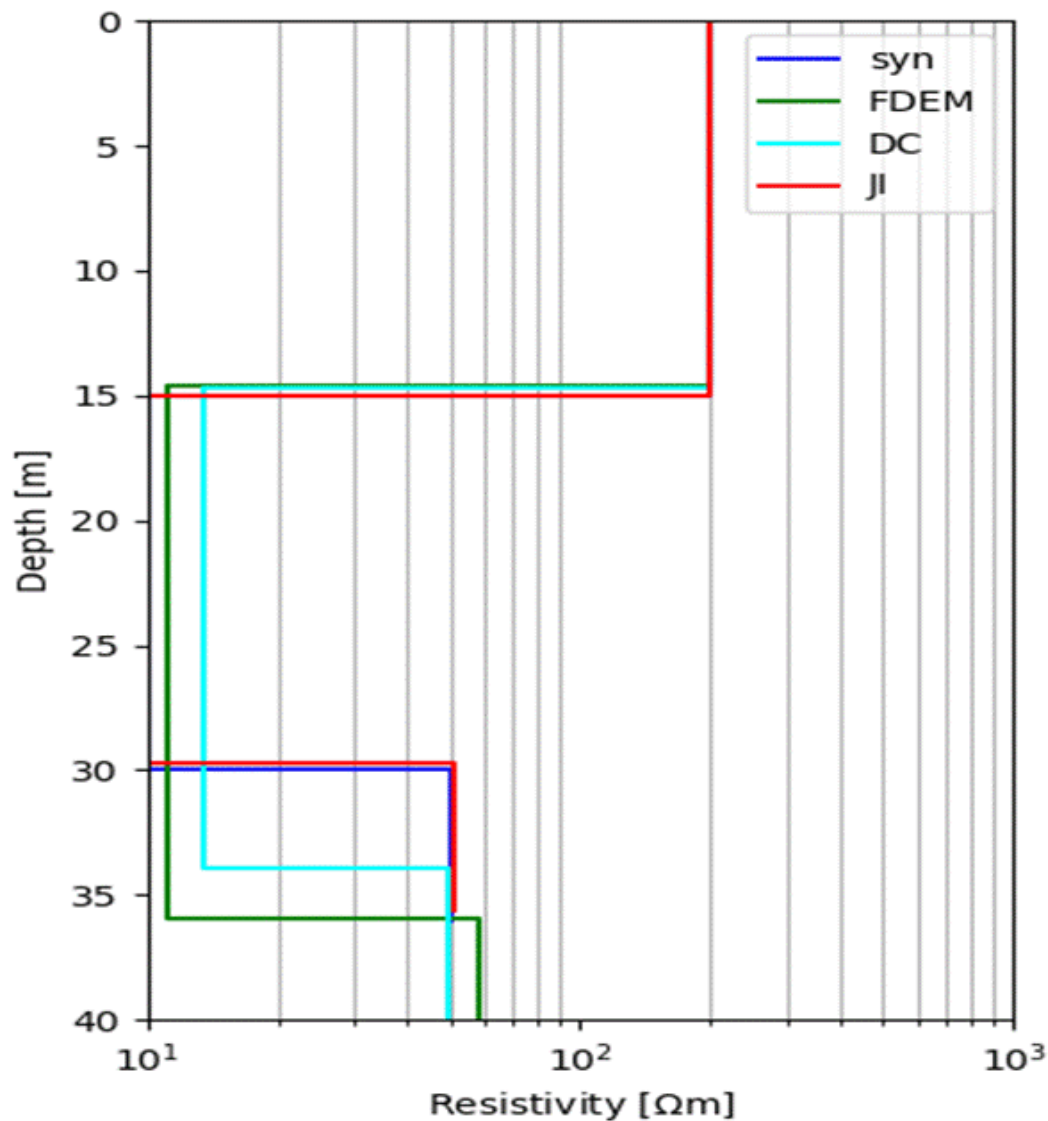


Fig. 1: Model of resistivity with depth.

The model predicts a shallow structure with a high resistivity of around 198.35 m above the depth of 15 m, which could be limestone (10–10,000 m) or gravel (10–10,000 m), and a shallow structure with a low resistivity of 11.08 m below 15 m, which could be weathered or altered granite (1–100 m) and freshwater (10–100 m).

The FDEM response, shown in Fig. 2, demonstrates that the FDEM and DCEM data generated from synthetic data include two components: the primary magnetic field (IP) and the secondary magnetic field (OP), respectively. The model result is corroborated by the electromagnetic field's intersection of the OP and IP components, which has a

positive percentage of about 12.22% at a frequency of about 1.76KHz.

The curve for the three-layer model with a predominance of the H-type curve is shown in Fig. 3 (lines 1 through 3). This kind of curve is typically found in hard rock terrains, which are composed of three layers: dry topsoil with a high resistivity as the first layer, weathered rock with a low resistivity due to water saturation as the second layer, and compact hard rock with an extremely high resistivity as the third layer. In this instance, the resistivity values of the first layer are approximately 47.2 KHz, the second layer is approximately 30.2 KHz, and the third layer is approximately 198.7 KHz.



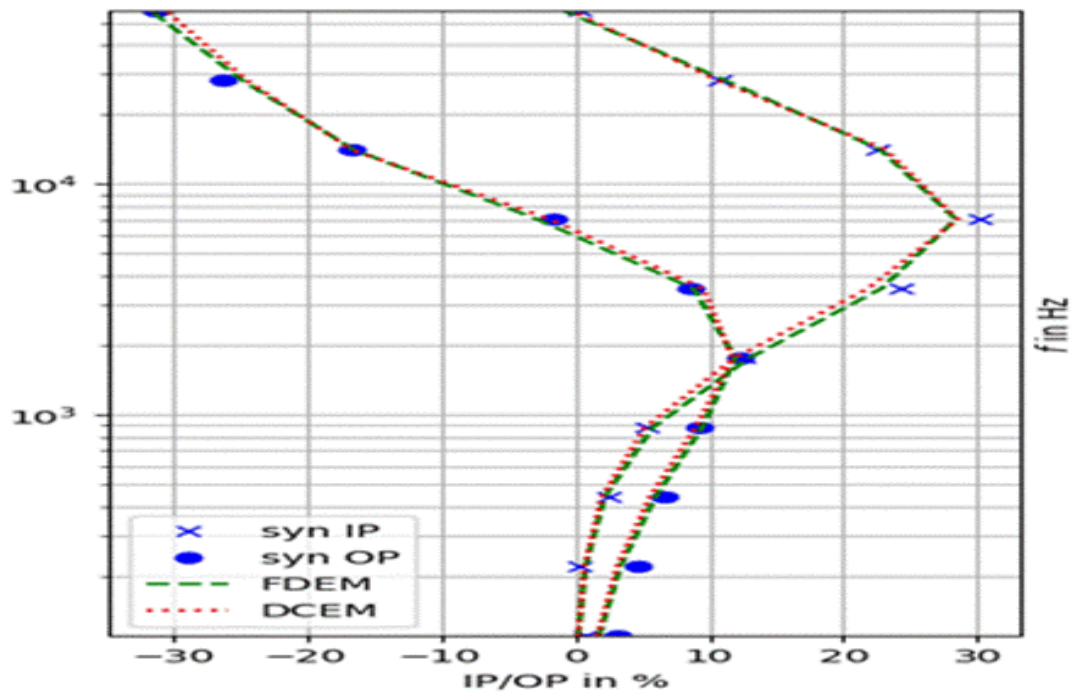


Fig. 2: FDEM response.

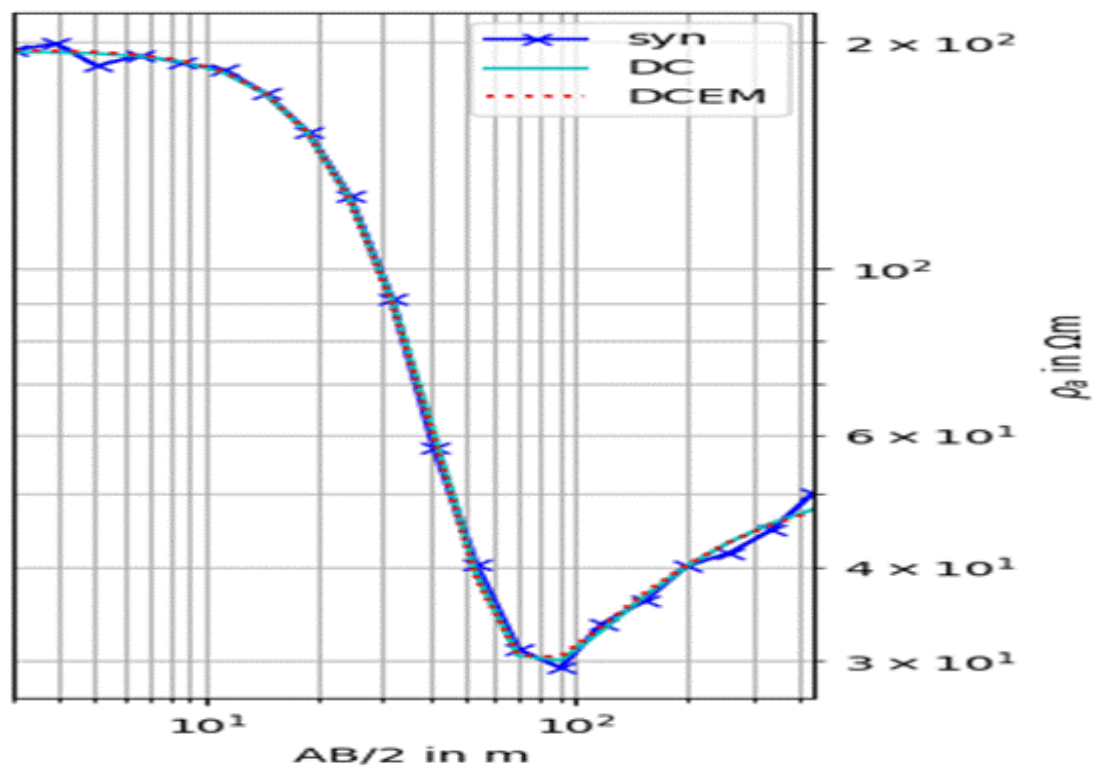


Fig. 3: Resistivity curve

||



#### 4.0 Conclusion

This piece of work aims to describe the joint inversion of electromagnetic and direct current measurements using artificial data derived from a Python-designed script. It has been discovered that subsurface models of the earth created using two or more geophysical approaches are more trustworthy than those created using just one. By integrating the datasets, transformations, and related errors, we were able to invert the DC and FDEM jointly using the joint forward operator. The combined use of electrical and electromagnetic approaches was found to be helpful for a better understanding of the subsurface electrical resistivity structure, as shown in Figs. 1, 2, and 3. Combining different methods made it possible to detect thin buried layers (conductive and resistive), which may be challenging to detect with just one method. As a result of the computational errors being significantly lower than those associated with the separate inversions of the individual geophysical datasets, it is concluded that the joint inversion of direct current and frequency domain electromagnetic sounding provided a more accurate representation of the subsurface.

Other computer languages should be used to provide models that are comparable to those already produced, which can provide opportunities for improved applications.

c) Synthetic data from other electromagnetic methods, such as time domain electromagnetic (TDEM), transient electromagnetic (TEM), telluric (T), and magnetotelluric (MT), should be jointly inverted with synthetic direct current electrical resistivity sounding to produce models that can be compared to the ones developed in this research work for further studies.

#### 5.0 References

Appa-Rao, A. & Roy A. (1973). Field results for direct current resistivity profiling with two electrode array. *Geoexpl.* 11, pp. 21–44.

Buselli, G., Barber C., Davis, G. B. & Salama, R. B. (1990). Detection of

groundwater contamination near waste disposal sites with transient EM and E methods. *Geotechnical and Environmental Geophysics, V. 2, Environmental and groundwater, Society of Exploration geophysicist, , 27–39.*

Gao G., Abubakar A., & Habashy T. M. (2012). Joint inversion petrophysical inversion of electromagnetic and full-waveform seismic data. *Geophysics*, 77, pp. 3-18, <https://doi.org/10.1190/geo2011-0157-1>.

Keller G. V. (1992). Electrical and electromagnetic methods in areas of complex geology, *J. App. Geophys.* 29, pp. 181–192.

Nabighian M. N. (1991). *Electromagnetic methods in applied geophysics, 2, Applications, Society for Exploration Geophysicist*, [https://doi.org/10.1190/1.9781560802631\\_fm](https://doi.org/10.1190/1.9781560802631_fm)

Ohaeguchu, H. E, Anyadiegwu F. C, Odoh P. O. & Orji F. C (2019). Review of top notch electrode arrays for geoelectrical resistivity surveys. *J. Nig. Soc. of Physical Sciences*, 1, 4, pp. 147-155.

Verma, R. K. & Mallick, K. (1979). Detectability of intermediate conductive and resistive layers by ime domain electromagnetic sounding. *Geophysics* 44, pp.1862-1878.

Verma, S. K. & Sharma, S. P. (1993). Resolution of thin layers using joint inversion of Electromagnetic and direct current resistivity sounding data. *J. Electromag. Waves and Appl.* 7, pp. 443–479.

Zhang, R. & Li, T. (2019). Joint inversion of 2D gravity gradiometry and magnetotelluric data in mineral exploration. *Minerals* 9(9).

Zhdanov, M. S. & Keller, G. V. (1994). The geoelectrical methods in geophysical exploration. *Methods in Geochemistry and Geophysics* 31, 873, <https://doi.org/10.1063/1.5042874>.



**Consent for publication**

Not Applicable

**Availability of data and materials**

The publisher has the right to make the data public

**Competing interests**

The authors declared no conflict of interest. This work was carried out in collaboration among all authors.

**Funding**

There is no source of external funding

**Authors' contributions**

E. Ohaegbuchi designed the python algorithm used for the research. B. I. Ijeh provided guidance on the research methodology. M. I. Ojiaku assisted with the literature review and interpretation of results.

